doi:10.1016/j.jmb.2009.02.056 J. Mol. Biol. (2009) xx, xxx–xxx

JMB

Available online at www.sciencedirect.com
ScienceDirect

ELSEVIER

Human Neuroserpin: Structure and Time-Dependent Inhibition

Stefano Ricagno[1]†, Sonia Caccia[2]†, Graziella Sorrentino[1], Giovanni Antonini[3] and Martino Bolognesi[1]*

[1]*Department of Biomolecular Sciences and Biotechnology, CNR-INFM and CIMAINA, University of Milano, Via Celoria 26, 20133 Milan, Italy*

[2]*Department of Biomedical Sciences and Technology, University of Milano, Via F.lli Cervi 93, I-20090 Segrate (MI), Italy*

[3]*Department of Biology, Interdepartmental Laboratory of Electronic Microscopy, University of Roma "Tre", Viale Marconi 446, I-00146 Rome, Italy*

Received 21 January 2009; received in revised form 19 February 2009; accepted 24 February 2009

Edited by R. Huber

Human neuroserpin (hNS) is a protein serine protease inhibitor expressed mainly in the nervous system, where it plays key roles in neural development and plasticity by primarily targeting tissue plasminogen activator (tPA). Four hNS mutations are associated to a form of autosomal dominant dementia, known as familial encephalopathy with neuroserpin inclusion bodies. The medical interest in and the lack of structural information on hNS prompted us to study the crystal structure of native and cleaved hNS, reported here at 3.15 and 1.85 Å resolution, respectively. In the light of the three-dimensional structures, we focus on the hNS reactive centre loop in its intact and cleaved conformations relative to the current serpin polymerization models and discuss the protein sites hosting neurodegenerative mutations. On the basis of homologous serpin structures, we suggest the location of a protein surface site that may stabilize the hNS native (metastable) form. In parallel, we present the results of kinetic studies on hNS inhibition of tPA. Our data analysis stresses the instability of the hNS–tPA complex with a dissociation half-life of minutes compared to a half-life of weeks observed for other serpin–cognate protease complexes.

Keywords: FENIB; neuroserpin; neurodegeneration; protein protease inhibitor; tissue plasminogen activator

Introduction

Human neuroserpin (hNS), a member of the serpin (serine protease inhibitor) superfamily,[1] is mainly expressed in neurons, but hNS mRNA has been detected in the pancreas, heart, and testis.[1,2] Human neuroserpin (SERPINI1 according to the accepted serpin nomenclature[3]) is a secretory protein that exerts its recognized physiological role in axonogenesis and synaptogenesis, during development and in synaptic plasticity in the adult, both as an inhibitor of tissue-type plasminogen activator (tPA) and in a tPA-independent way.[1,2,4,5] In Alzheimer's disease models, hNS has been found to interact with the β-amyloid (Aβ) peptide with remarkable effects: first, interaction with Aβ depresses the hNS protease inhibitory activity, and second, Aβ amyloid aggregation is enhanced. Moreover, in cell lines and in a *Drosophila* model, hNS exerts a protective role against the toxicity of Aβ peptide aggregates.[6]

Serpins are ubiquitous proteins (composed of 350–450 amino acids) whose fold is conserved through the phyla.[3] Their tertiary structure is characterized by three β-sheets (A, B, and C), nine main α-helices, and a long exposed flexible loop, the reactive centre loop (RCL),[3,7] which binds to the target protease active site. When the serpin–protease inhibitory complex is achieved, the protease recognizes the RCL as a pseudo-substrate and cleaves it at the P1–P1′ peptide bond,[8] with formation of a covalent acyl–enzyme adduct. RCL cleavage triggers a major conformational

*Corresponding author. E-mail address: martino.bolognesi@unimi.it.

† S.R. and S.C. contributed equally to this work.

Abbreviations used: hNS, human neuroserpin; tPA, tissue plasminogen activator; RCL, reactive centre loop; FENIB, familial encephalopathy with neuroserpin inclusion bodies; IPR-pNA, H-D-Ile-Pro-Arg-*p*-nitroanilide; PAI-1, plasminogen activator inhibitor-1; VR-1, tPA variable region-1; EFK-pNA, Pyro-Glu-Phe-Lys-*p*-nitroanilide.

0022-2836/$ - see front matter © 2009 Published by Elsevier Ltd.

change within the serpin molecule; before hydrolysis of the acyl–enzyme, the RCL upstream of the scissile bond is inserted between strands 3 and 5 of the A β-sheet as strand 4 (s4A; strands and helices are identified by the "s" and "h" suffixes, respectively). As a consequence, the protease, covalently bound to the P1 residue, is transferred to a serpin surface region (about 70 Å away) opposite to the location of the intact RCL. Such extensive structural changes result in inhibition of the protease through deformation of the catalytic triad that dramatically slows the deacylation step (typically weeks).[9] The hNS–tPA inhibitory interaction, however, differs from such a general scheme in that the acyl–enzyme intermediate is relatively short-lived.[10]

In addition to native and cleaved states, selected serpins are known to adopt an inactive "latent" conformation where, in the absence of proteolytic cleavage, the intact RCL is fully inserted into sheet A as s4A (for a review, see Ref. 11). Several pieces of evidence show that in selected serpins the stability of the native *versus* the latent form can be increased by the interaction with polypeptides binding to the s1A and hE regions. Plasminogen activator inhibitor-1 (PAI-1) converts into the latent state if the cofactor protein vitronectin is unavailable,[12] and the bacterial serpin tengpin adopts native or latent forms depending on the intramolecular interaction of its N-terminal region with the s1A-hE motif.[13]

The first disease shown to be associated to serpin polymerization was discovered in 1992 and was related to an unstable form of α1-antitrypsin, which accumulates as polymeric aggregates in hepatocytes, eventually leading not only to cirrhosis but also to lung emphysema, α1-antitrypsin being a natural inhibitor of neutrophil elastase.[14] Two aspects of pathology are therefore related to serpin polymerization: the damage occurring at a local level due to polymer accumulation at the site of protein synthesis, and more general effects resulting from a distributed lack of serpin inhibitory activity. It is now recognized that different serpins can form long linear polymers, leading to intracellular accumulation and diseases, collectively reported as "serpinopathies".[1,15] The structural bases for serpin polymerization have been under scrutiny for more than 15 years, resulting in two primary models, both essentially based on swapping of protein elements and on the instability of the main serpin β-sheet. On one hand, it was proposed that formation of polymeric serpin would involve the repeated incorporation of part of the RCL from one molecule into the A β-sheet of the following one.[14] On the other hand, based on the crystal structure of a dimeric form of antithrombin, a model has been recently proposed whereby iterative domain swapping, based on the intermolecular exchange of strands s4A and s5A, would lead to formation of a string of domain-swapped latent molecules.[16,17] Such a model requires a partially unfolded polymerogenic intermediate (M∗) whose helix I, strand s5A, and the connecting loop are unstructured and solvent-exposed.[16] The M∗ intermediate would then associate with linear polymers by inserting part of its unstructured region (equivalent of two β-strands) into a widened A β-sheet of the neighboring molecule. Both models agree on the fact that serpin polymers are composed of individual protein molecules that retain much of their native state, different from amyloid fibrils, where a considerable level of native protein unfolding is held to be present.

Human neuroserpin is responsible for a polymerization-linked severe neurodegenerative disease, known as familial encephalopathy with neuroserpin inclusion bodies (FENIB).[1,15] Four pathological hNS single-site mutants have been described (S49P, S52P, H338R, and G392E) and are associated with various levels of dementia, progressive myoclonus epilepsy, dysarthia, and chorea.[18] They are held to enhance hNS propensity to polymerize and form bulky deposits in the endoplasmic reticulum and lysosomes.[19–21] The mutations correlate with *in vitro* polymerization rates, the extent of brain inclusions, and different levels of disease severity, with the earliest FENIB onset (associated to the G392E mutant) being typical of the first decade of life.[22]

Despite the considerable medical interest in hNS, to date only a 3.06 Å resolution structure of cleaved mouse neuroserpin has been reported.[23] Such lack of direct structural information prompted us to investigate the crystal structures of hNS in its native and cleaved forms, reported here at 3.15 and 1.85 Å resolution, respectively. Moreover, although the instability of the hNS–tPA complex over time had been previously recognized, the relative lack of kinetic studies taking into account the limited temporal stability of the complex for the analysis of the data led us to reconsider an investigation on tPA inhibition kinetics. The main molecular properties of hNS, such as RCL flexibility, RCL-dependent intermolecular interactions, potential interaction sites, the effects of FENIB mutations on hNS stability, and the hNS transient inhibitory process, are discussed in the light of the reported results.

Results

Overall fold of native neuroserpin

Human neuroserpin has been crystallized (as the intact active metastable form, residues 1–410) in the orthorhombic *I*222 space group, with five molecules per asymmetric unit (chains A through E). The crystal structure of native hNS has been solved at 3.15 Å resolution, yielding a good-quality model as judged by commonly accepted criteria (see Table 1). Interpretable electron density is available, with some local discontinuities, for amino acids Pro22 through Met 400, for all five independent molecules. As for all known serpins crystallized in the native metastable form, hNS displays the typical serpin fold composed of three large β-sheets and nine α-helices; sheet A consists of five β-strands, while the RCL (between strands s3A and s1C) largely

Please cite this article as: Ricagno, S. *et al.*, Human Neuroserpin: Structure and Time-Dependent Inhibition, *J. Mol. Biol.* (2009), doi:10.1016/j.jmb.2009.02.056

Table 1. Data collection and refinement statistics for native and cleaved hNS structures

	Native hNShuman neuroserpin	Cleaved hNShuman neuroserpin
Beam line	ESRF ID14-2	ESRF ID14-1
Space group	$I222$	$P2_12_12$
Unit cell (Å)	$a=171.8$, $b=179.2$, $c=248.2$	$a=72.93$, $b=100.06$, $c=115.82$
Solvent content (%)	75	55
Resolution (Å)	20–3.15	40–1.85
R_{sym} (%)	12.9 (83.4)	9.9 (65.8)
$I/\sigma I$	10.3 (1.9)	12.7 (2.7)
Completeness (%)	99.6 (100.0)	99.9 (99.9)
Redundancy	4.1 (4.2)	7.1 (6.5)
Unique reflections	66,051	78,887
Refinement		
R_{work} (%)	23.5	19.2
R_{free} (%)	28.6	23.9
No. of atoms		
Protein atoms	14,432	5882
Water molecules	—	541
Ramachandran plot		
Most favoured region (%)	92.6	96.35
Allowed region (%)	2.5	3.22
Outliers (%)	1.4	0.44

Values in parentheses are for the highest-resolution shells: 3.15–3.32 and 1.85–1.95 Å.

[a] $R_{merge}=\sum|I-\langle I\rangle|/\sum|I|$, where I is the observed intensity and $\langle I\rangle$ is the average intensity.

[b] $R_{work}=\sum_{hkl}||F_o|-|F_c||/\sum_{hkl}|F_o|$ for all data except 5% that were used for R_{free} calculation.

protrudes from the protein core, showing no interaction with sheet A (Fig. 1a).

In all five independent hNS molecules (Fig. 1c) no electron density is observed for the loops located between helices hC and hD (residues 79–85) and between strands s1B and s2B (residues 231–238). Helix hD can be unambiguously traced; however, the electron density is of poor quality and its higher than average *B*-factors reflect particular flexibility or local disorder. Except for chain B, all the other four hNS chains show incomplete electron density for their RCLs. In particular, chain E displays poorer electron density relative to the other four independent molecules, probably due to its contained contacts within the crystal lattice (Supplementary data). The five hNS chains display very similar overall conformations: molecules A, B, D, and E superpose with an RMSD lower than 0.6 Å (Table 2) calculated over the whole C^{α} backbone, with the exclusion of the RCLs whose conformations vary in the five independent hNS molecules (Fig. 1d). Structural superposition of the hNS C chain on the other four chains results in slightly higher RMSDs (0.7–0.8 Å) due to the different conformations adopted by helices hG and hH in chain C (Table 2 and Supplementary data).

Crystal packing of native neuroserpin

The five independent hNS molecules hosted in the crystal asymmetric unit are held together mainly via RCLs and the C β-sheet, being assembled in a star-like pentamer at the centre of which the RCLs converge and are partly solvent-inaccessible (Fig. 1c). The RCL hosts several low-polarity residues (15 out of 20) whose hydrophobic association (particularly in the C-terminal half of the RCL) is likely driving the association to the observed pentamer. On the other hand, RCL hydrophobicity may also be one of the factors promoting hNS polymeric aggregation, since, according to the current models, linear hNS polymers require partial insertion of part of the RCL in the A sheet of a neighboring hNS molecule.[11]

Reactive centre loop

Each RCL in the five independent hNS chains displays a different conformation (Fig. 1d), such that none of the five RCLs can be properly superposed on any other. The N-terminal part of all five RCLs (residues 348–357) does not establish intra/intermolecular interactions, in keeping with the conformational disorder observed for this stretch in chains C and E. The C-terminal part of all RCLs is instead buried in the pentamer association centre (Fig. 1c) and clearly defined in the electron density.

The C-terminal part of chain A RCL is of particular interest since strand s1C extends into the RCL (residues 363–367), establishing intermolecular hydrogen bonds with a similarly elongated s1C strand from molecule D (residues 365–368). Together with residues 227–230 of chain C (i.e., s1B) they form an intermolecular, antiparallel, three-stranded β-sheet that helps to stabilize part of the pentameric assembly (Supplementary data).

Human neuroserpin chain B shows interpretable electron density for the whole RCL, whose C-terminal part interacts with strand s1C from chain C, with residues 259–261 from chain A (s3B-hG loop), and with the RCL from chain D (residues 363–373). Similarly, the interactions between the RCL from chain B (364–367) and the RCL from chain D (360–362) result in β-like intermolecular structure. The above observations show that the RCL sequence allows wide conformational variability and stress the RCL's strong adaptability to intermolecular interactions that may also find partners other than the hNS A sheet.

s1A intermolecular interactions

An elongated electron density feature extending for about 12 Å is visible adjacent to strand s1A for every native hNS chain, being of particularly good quality in chain B. The extra density can be properly fitted by residues 400–407 from the C-terminus of the B chain from a symmetry-related pentamer (Fig. 2). The interaction between s1A and the C-terminus of an adjacent chain is reminiscent of what has been observed for tengpin and for PAI-1, where interactions of s1A with the N-terminus (in tengpin) and with vitronectin (in PAI-1) stabilize the native metastable serpin conformation *versus* the

Please cite this article as: Ricagno, S. *et al.*, Human Neuroserpin: Structure and Time-Dependent Inhibition, *J. Mol. Biol.* (2009), doi:10.1016/j.jmb.2009.02.056

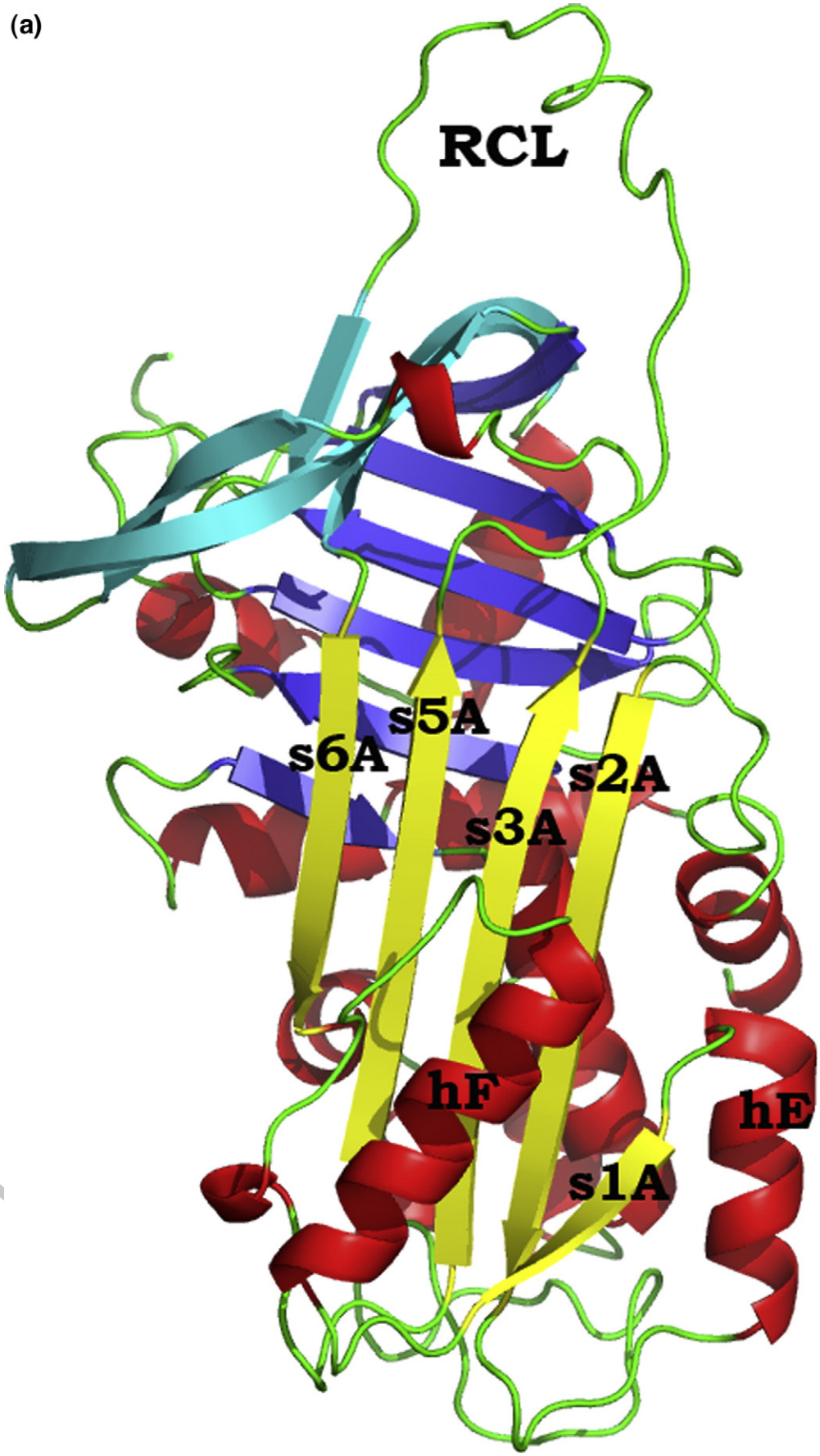

Fig. 1 (*legend on next page*)

Please cite this article as: Ricagno, S. *et al.*, Human Neuroserpin: Structure and Time-Dependent Inhibition, *J. Mol. Biol.* (2009), doi:10.1016/j.jmb.2009.02.056

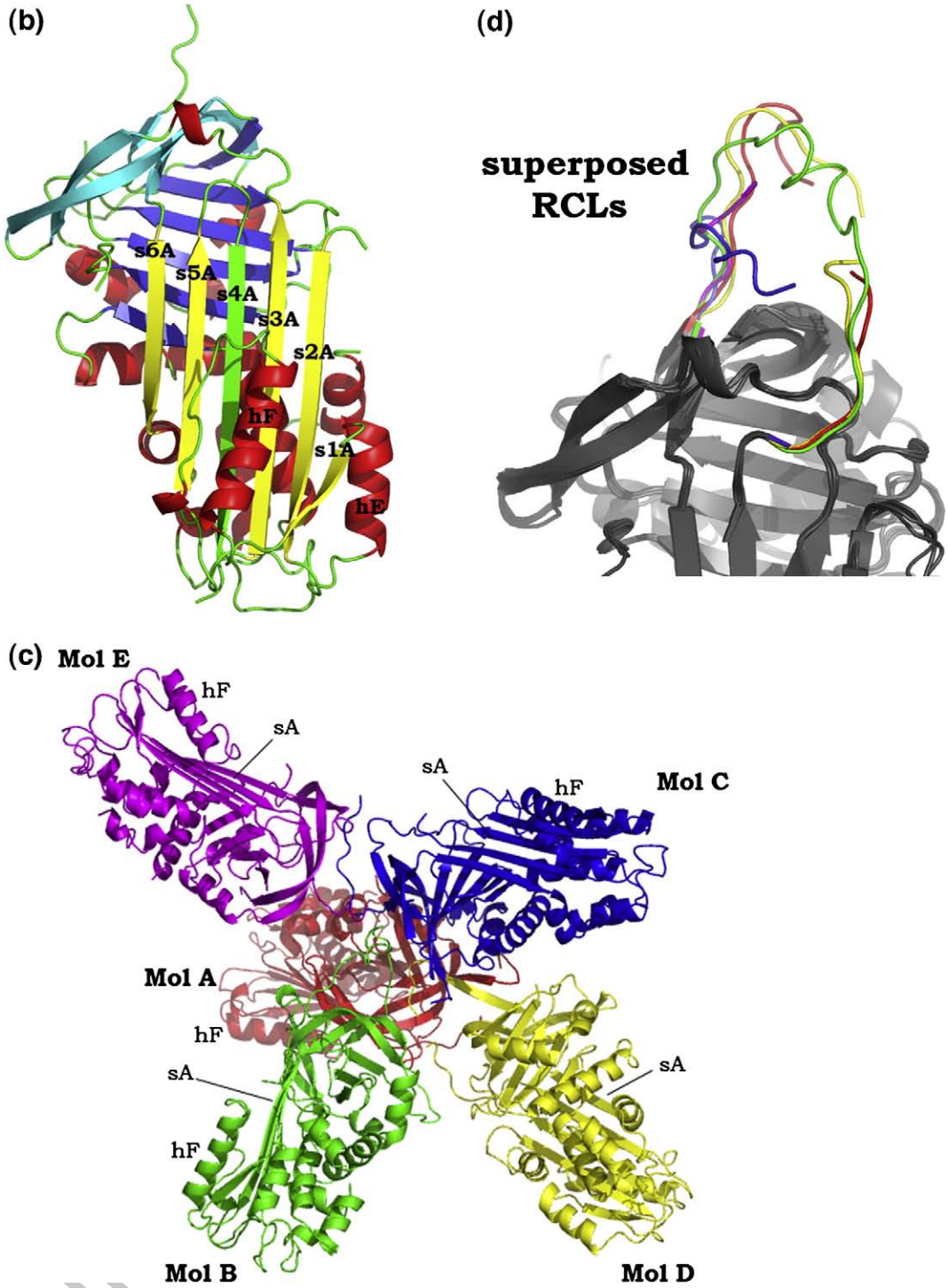

Fig. 1. (a) Cartoon representation of native hNS (chain B). Sheet A is shown in yellow, sheet B in blue, and sheet C in cyan. α-Helices are red and loops are green. (b) Cartoon representation of cleaved hNS coloured as in (a); the RCL inserted into sheet A is green. (c) Cartoon representation of hNS crystallographic pentamer. The RCLs are located at the centre of the pentameric assembly. For reference, when visible in the drawn chains, helix F (hF) and sheet A (sA) are labelled. (d) Cartoon representation of part of the five superposed hNS chains (grey) neighboring the RCL region; chain A RCL is shown in red, chain B in green, chain C in blue, chain D in yellow, and RCL E in magenta.

latent form.[12,13] Such finding may suggest that the s1A region requires stabilization for hNS to maintain the native metastable conformation (stable for weeks at 20 °C before crystallization occurs).

Overall structure of cleaved neuroserpin

The structure of trypsin-cleaved hNS was solved and refined at 1.8 Å resolution (R_{work} 19.2%, R_{free}

Please cite this article as: Ricagno, S. *et al.*, Human Neuroserpin: Structure and Time-Dependent Inhibition, *J. Mol. Biol.* (2009), doi:10.1016/j.jmb.2009.02.056

Table 2. RSMD values calculated between native hNS chains A–E

	A (364)	B (376)	C (358)	D (361)	E (340)
A	—	0.6 Å (350)	0.75 Å (330)	0.44 Å (355)	0.47 Å (333)
B		—	0.85 Å (327)	0.64 Å (352)	0.49 Å (330)
C			—	0.72 Å (328)	0.80 Å (320)
D				—	0.46 Å (330)
E					—

The number of C^{α} atoms for each chain is in parentheses in the top row. The number of C^{α} atoms used to calculate each RSMD value is specified for each comparison.

23.9%) (Table 1). The three main β-sheets and nine α-helices typical of other cleaved serpins are readily recognized in the proteolyzed hNS structure (Fig. 1b). The two hNS chains hosted in the asymmetric unit are structurally very similar, with an RMSD of 0.31 Å calculated over the whole C^{α} backbone. Both independent chains were unambiguously traced in the electron density between residues 24 and 400, with only a few gaps of low or absent electron density. Interestingly, helix hD is only partially visible, is characterized by higher than average *B*-factors (about 35 $Å^2$), and is isolated from the rest of the molecule by two electron density gaps (81–85 and 94–102). Notably, the Peptide Cutter server‡ predicts two highly probable trypsin cleavage sites in the two gap regions. It is possible that hD, even if cleaved, can be non-covalently associated with the rest of the hNS molecule; however, it should be recalled that hD displays poor electron density also in the native hNS structure.

As expected, the RCL is cleaved at residue 362 and inserted in the A β-sheet as β-strand 4 (residues 347–361). Arg362, the P1 RCL residue, can be recognized at the lower edge of β-sheet A (Fig. 1b). The C-terminal part of the cleaved RCL (residues 365–368) remains located next to the site it occupies in the uncleaved hNS, being stabilized by crystal contacts to the distal part of sheet A from a symmetry-related chain.

A DALI search shows that the cleaved serpin structure most similar to hNS is antithrombin III, with an RMSD of 1.3 Å for 351 of 410 C^{α} pairs [Protein Data Bank (PDB) code 1ATT]. Cleaved PAI-1 shows an RMSD of 2.1 Å for 352 of 379 C^{α} pairs (PDB code 9PAI). Conversely, the superposition between cleaved hNS and α1-antitrypsin in complex with trypsin (PDB code 1EZX) yields an overall RMSD of 1.47 Å for 309 C^{α} pairs, and the region interacting with trypsin shows the lowest RMSD.

Neuroserpin inhibitory activity

The hNS inhibitory activity on tPA was analyzed by means of a chromogenic assay using the tPA substrate H-D-Ile-Pro-Arg-*p*-nitroanilide (IPR-pNA). Serpins typically show inhibition progress curves characteristic of slow-binding inhibitors, reaching a plateau after pre-steady-state release of the product, as expected for an irreversible inhibitory complex.[24,25] On the contrary, immediately following the initial phase typical of slow-binding inhibitors, the progress curves for the hydrolysis of IPR-pNA by tPA in the presence of hNS show a progressive increase in the rate of substrate hydrolysis (Fig. 3a), revealing a recovery of tPA activity after transient inhibition by hNS. Such behavior suggests instability of the hNS–tPA acyl–enzyme complex, with functional tPA rescue following deacylation. Fitting of the progress curves by numerical integration according to the mechanism drawn in reactions 1 and 2 [Eq. (1)] yielded a k_{inh} value of $(2\pm0.06)\times10^5\ M^{-1}\ s^{-1}$, with a rate constant of $(1.2\pm0.03)\times10^{-3}\ s^{-1}$ for complex breakdown, corresponding to a dissociation half-life of about 10 min. Thus, despite a relatively efficient rate of inhibition, hNS cannot be considered a stable tPA inhibitor. Such peculiar instability of the hNS–tPA complex, compared to the much longer half-life of other serpin–protease complexes (usually weeks), had previously been reported.[10,26] Notably, however, the models previously used for fitting the experimental data did not take into account the recovery of protease activity, describing only the initial part of the reaction (the build-up of inhibition), thus leading to rate constant values quite different from those reported here.[2,5,26]

To complement the above data analysis with an independent assessment, the products of the hNS–tPA reaction were separated and quantified by SDS-PAGE, followed by fluorescent staining (Fig. 3b). Such an approach showed that the serpin–protease complex band (~75 kDa) remained stable for an initial period of time, after which it gradually started to fade away. In parallel, a decrease in intensity of the intact hNS band (~45 kDa) and an increase of a ~40-kDa band corresponding to cleaved hNS were observed, suggesting the ongoing hNS–tPA complex deacylation. All the hNS present was eventually cleaved with no evidence of residual latent hNS form. The fluorescence intensity data corresponding to the intact, complexed, and cleaved hNS were interpolated according to the neuroserpin inhibition mechanism (Materials and Methods; reaction 1). The resulting rate constant values matched quite satisfactorily those obtained from the chromogenic assays, such that a common set of values for the rate constants was obtained (Supplementary data). The chromogenic and SDS-PAGE assays were completely reproducible when the protease domain of tPA alone was used (data not shown), suggesting that the short-lived stability of the acyl–enzyme complex is not due to the tPA light chain preventing insertion of the RCL into sheet A, thus hampering protease translocation after the P1–P1′ bond cleavage.

Lastly, in order to combine the transient nature of hNS inhibitory activity with tPA physiological activation of plasminogen, we performed an indirect assay in which plasminogen activation by tPA in the presence of hNS was monitored via the hydrolysis of a chromogenic substrate specific for plasmin. As

‡ http://www.expasy.ch

Please cite this article as: Ricagno, S. *et al.*, Human Neuroserpin: Structure and Time-Dependent Inhibition, *J. Mol. Biol.* (2009), doi:10.1016/j.jmb.2009.02.056

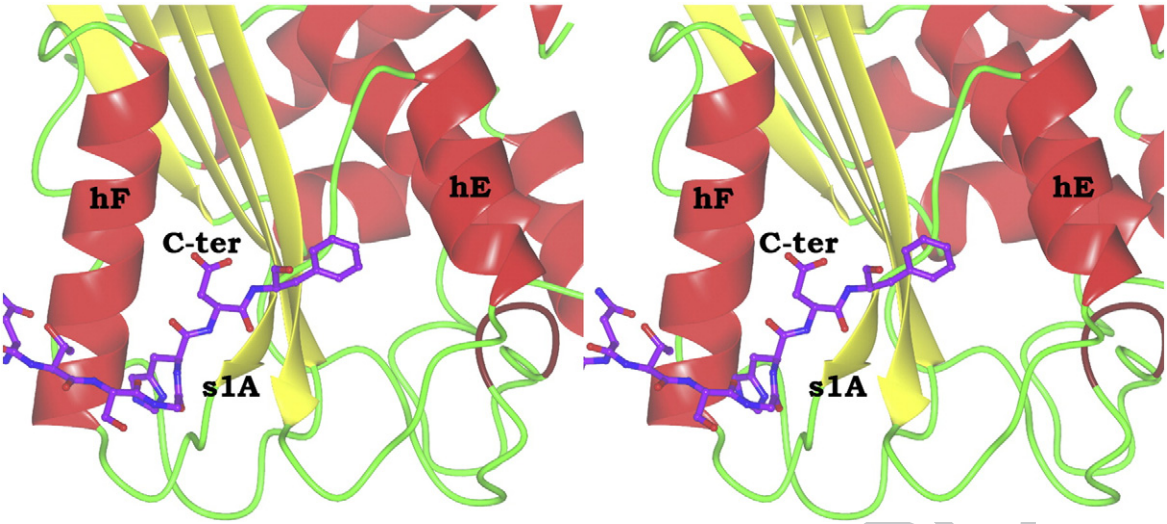

Fig. 2. Stereo cartoon of the hF-s1A-hE region from molecule B in the native hNS structure, coloured according to secondary structures. The C-terminus from the symmetry-related molecule B∗, shown as purple sticks, interacts with s1A. In particular, the side chain of His 405 is inserted between hF and s1A.

shown in Fig. 3c, plasminogen activation is delayed due to the presence of hNS, although the serpin is readily cleaved by both tPA and plasmin (Supplementary data).

Discussion

Here we report the first X-ray structural characterization of hNS. Two main hNS forms are described: the native active hNS, at 3.15 Å resolution, showing an intact, solvent-exposed RCL, and the cleaved form, at 1.85 Å resolution, showing the RCL upstream of the P1–P1′ cleavage site inserted in sheet A.

Native hNS is observed in the crystal lattice as a pentameric assembly whose core buries part of each RCL, providing most of the pentamer-stabilizing intermolecular (hydrophobic) interactions. Within the pentamer, the individual hNS chains display interaction surfaces (average, 11.2% of the total chain surface) much larger than "interpentameric" interaction surfaces (about 5.8%), suggesting the pentamer role as the crystal lattice building block (Supplementary data). Despite the tendency of hNS solutions to yield higher-order polymeric species with aging, hNS crystals have been obtained in our laboratory under more than 20 non-redundant crystallization conditions over periods of weeks. All hNS crystals display the same morphology, and all the crystals tested share the same orthorhombic space group and unit cell constants (Table 1), indicating that the pentameric assembly is maintained under several different hNS crystallization conditions.

Various examples of RCL ability to form intermolecular β-like interactions are observed in the hNS native structure. RCLs from chains A and D together with strand s1B from chain C form a three-stranded β-sheet (Supplementary data). RCLs from chains D and B also establish β-like interactions. All such intermolecular interactions have important implications: (i) RCL displays evident propensity to form β-strands outside sheet A; (ii) RCL hydrophobicity and tendency to form β structure promote intermolecular RCL interactions; (iii) by using the intact RCL properties, hNS may assemble into reversible (non-pathological) oligomers, that can promptly release monomeric hNS for tPA inhibition. It is worth noting that hNS is found *in vivo* to be secreted in dense-cored secretory granules, where its concentration is high and hNS is stored in a native non-polymeric form.[27]

Recently, two serpins, PAI 1 and tengpin, have been shown to host an allosteric site in the s1A-hE region, where inter/intramolecular interactions control the switch between the latent and native conformations.[12,13] Sequence and structural comparisons show high levels of similarity between hNS and tengpin in this region. In particular, three residues shown to be relevant for the stability of tengpin's native conformation are conserved, or conservatively mutated, in hNS (tengpin/hNS: Leu159/Leu125, Ile162/Met128, Ile170/Val136) (Supplementary data). In the hNS native structure, but not in the cleaved form, the C-*termini* of symmetry-related molecules extensively interact with s1A. The protein fragment ligated to s1A may act as a constraint on the edge of sheet A and prevent it from widening, thus hampering intramolecular RCL insertion in the sheet (required for switching to latent conformation). Such an interaction, which would suggest the presence of an allosteric site also in hNS, will require mutational analyses and other experimental approaches to be validated. It is, however, in keeping with the results and structural interpretations reported for selected serpins.[12,13]

Please cite this article as: Ricagno, S. *et al.*, Human Neuroserpin: Structure and Time-Dependent Inhibition, *J. Mol. Biol.* (2009), doi:10.1016/j.jmb.2009.02.056

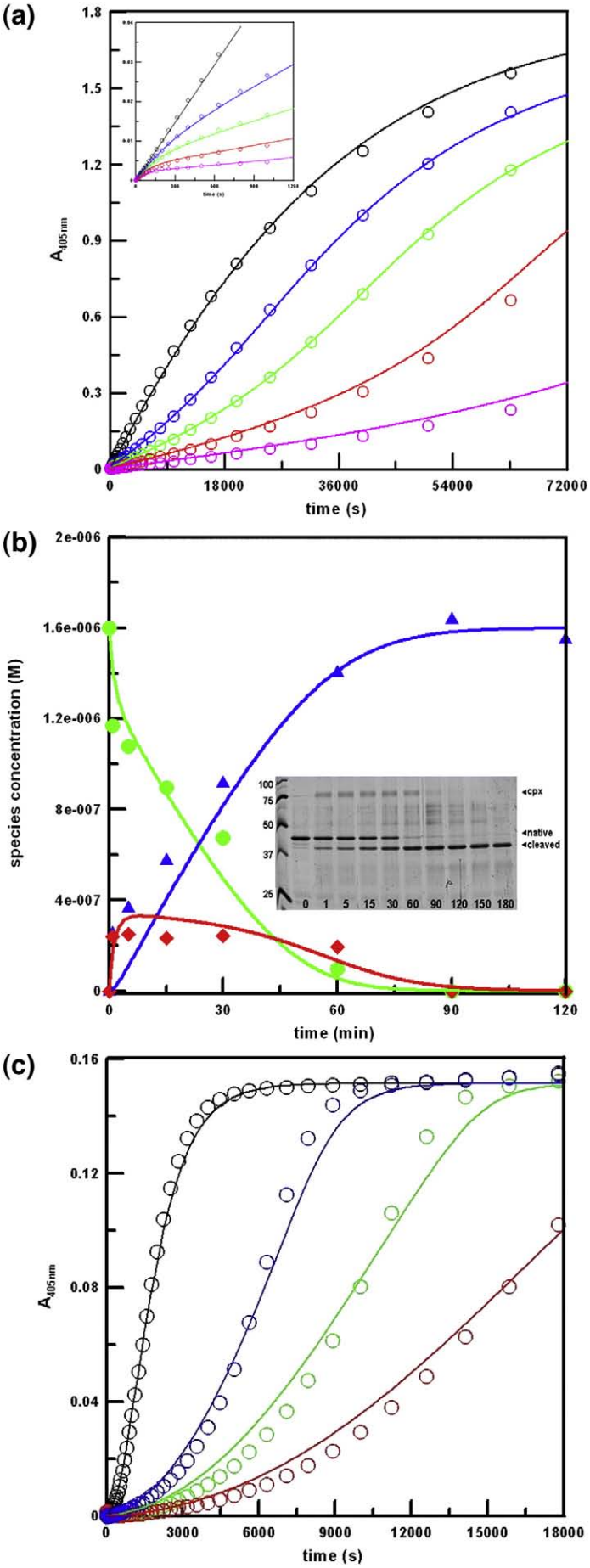

Fig. 3. (a) Progress curves of the hydrolysis of IPR-pNA (170 μM) by tPA (1 nM) in the presence of hNS (0, 15, 30, 60, and 120 nM). Inset: close-up view of the reaction between $t=0$ and 20 min. Symbols represent the experimental data, only part of which are indicated for clarity. Continuous lines are drawn according to the best-fit parameter values obtained from reactions 1 and 2. (b) hNS (1.6 μM) was incubated with tPA (0.4 μM). Band densities from SDS PAGE (inset), expressed as concentrations, were plotted against time: native (circles), RCL-cleaved (triangles), and complexed (diamonds) hNS. Continuous lines are drawn according to the best-fit parameter values obtained from reaction 1. Inset: lane 1, molecular marker; lane 2, hNS; lanes 3–11, 1-, 5-, 15-, 30-, 60-, 90-, 120-, 150-, and 180-min time points. Native, RCL–cleaved, and complexed (cpx) hNS bands are shown. (c) Progress curves of the hydrolysis of EFK-pNA (15 μM) by plasmin (initial concentration of plasminogen, 5 nM) following plasminogen activation by tPA (20 nM) in the presence of increasing concentrations of hNS (200, 400, 800 nM). Symbols represent the experimental data, only part of which are drawn for clarity, and the continuous lines are the fits of the reactions 1, 3, 4, and 5 described in Materials and Methods.

Please cite this article as: Ricagno, S. *et al.*, Human Neuroserpin: Structure and Time-Dependent Inhibition, *J. Mol. Biol.* (2009), doi:10.1016/j.jmb.2009.02.056

Intriguingly, all the three neuroserpin structures available to date (native and cleaved hNS from this report and cleaved mouse neuroserpin[23]) show a high degree of flexibility in the helix D region. The complete lack of electron density for the C–D helix region (residue 69–103) prompted us to speculate that, in trypsin-treated mouse neuroserpin, the protease cleaved other regions besides the P1 site, thus removing the 69–103 residue stretch.[23] Whether cleaved or not visible in the crystal structure, the C–D helix region is undoubtedly highly flexible in mouse neuroserpin. In the cleaved hNS structure, helix D is visible with short electron density gaps at the C- and N-terminal ends, while in the native structure, such helix is almost completely visible, but shows very high average *B*-factors. In both hNS structures, the loop connecting helix D to s2A is not defined by electron density. Such flexibility might suggest that this region is coded to bind a yet uncharacterized ligand, as observed in other serpins.[28]

Four single-site hNS mutants have been reported as associated with the FENIB pathological phenotype, with a direct correlation between the instability of the mutant and the severity of the symptoms.[18] All four mutations (S49P, S52R, H338R, and G392E) are known to promote polymerization. The four FENIB mutated residues are strongly conserved throughout the serpin superfamily (>90% conserved among all serpin structures, from humans to bacteria, present in the PDB). In the light of the recently proposed polymerization model[16] and considering the hNS crystal structures here reported, the effect of the pathological mutations can be rationalized (Supplementary data).

As described earlier and further detailed here, the kinetic behavior of the hNS–tPA complex differs markedly from the virtually irreversible inhibitory processes paradigmatically related to serpins. In fact, more properly, it resembles a substrate hydrolysis process with a delayed intermediate. The kinetic data analyzed here show that the half-life of the cleaved hNS–tPA complex is only 10 min. An immediate physiological consequence of this observation is that recognition of the hNS–tPA complex by receptors must occur in a matter of minutes for cellular internalization to take place. In fact, although no direct evidence of the hNS–tPA complex has been so far reported *in vivo*, cellular internalization, a process mediated by LRP receptor recognition, is observed in cell cultures both for active hNS and for the hNS–tPA complex.[29]

From a structural viewpoint, transient inhibition of tPA by hNS implies that the deformation of the protease active-site region (preventing the deacylation reaction) may not be as dramatic in hNS–tPA as reported for other serpin–protease complexes.[9] However, structural comparison between cleaved hNS and α1-antitrypsin in its covalent complex with trypsin[9] shows that the cleaved RCL is inserted in sheet A in the very same fashion in the two serpins, and the P1 residues (cleaved or linked to the protease, respectively) fall in the same surface locations. In this respect, recent reports have shown that stable acyl complexes require full insertion of the RCL,[30,31] while short-lived acyl complexes can be generated by improper RCL length[32] or by attractive interactions between the serpin and the protease.[33] Thus, the above observations suggest that the final conformation achieved by the RCL in cleaved hNS is unlikely to be responsible for the lower stability of the hNS–tPA complex.

The high affinity displayed by serpins for cognate proteases is determined not only by the nature of their P1 residue, but also by regions neighboring the active site and the RCL on the interacting surfaces of both macromolecules.[34] The tPA variable region-1 (VR-1, or 37-loop), an exposed loop rich in positively charged residues (Supplementary data), mapping near one edge of the active site, was recognized to be crucial for the interaction of tPA with PAI-1. The region of PAI-1 interacting with tPA VR-1 has been proposed to correspond to the negatively charged residues in the RCL region C-terminal to the cleavage site.[35,36] Differently from PAI-1, hNS does not display charged residues at that site; instead, a strong negatively charged patch is present in hNS on one side of β-sheet A (Supplementary data), which is absent in PAI-1. Upon cleavage, the bound protease must translocate toward the "lower rim" of the serpin molecule. Electrostatic interactions between the positive tPA VR-1 loop and the strongly negative hNS surface may lead to a decreased rate of tPA translocation. This would allow trapping of the hNS–tPA acyl complex into a relative energy minimum before the RCL is fully inserted into sheet A. Such intermediate steps would allow the protease to retain a structured active-site environment compatible with acyl complex hydrolysis and dissociation.

As a whole, our results provide an overview of hNS structural features and FENIB mutant instability in the light of the recent polymer formation theories, and provide foresight for mutational analyses of the hNS sites that may support maintenance of the native metastable form. The kinetic data presented, while in qualitative agreement with previous results, stress the short half-life of the hNS–tPA inhibitory complex, an uncommon property among serpins that opens new questions on its *in vivo* turnover.

Materials and Methods

hNS expression and purification

The plasmid coding for hNS with an N-terminal His-tag (kindly provided by Dr. Didier Belorgey, University of Cambridge, UK) was transformed in *Escherichia coli* Rosetta (DE3) pLys. Protein expression was carried out in SB broth (Athena system) at 17 °C overnight. hNS was purified by two-step chromatography. First, the crude cellular extract was applied onto a Ni-NTA Sepharose column (GE Healthcare) and hNS was eluted using a buffer containing 50 mM Tris–HCl, 300 mM NaCl, and 250 mM imidazole (pH 8.0). Second, size-exclusion chromatography was employed (Hi Load 16/60 Superdex

Please cite this article as: Ricagno, S. *et al.*, Human Neuroserpin: Structure and Time-Dependent Inhibition, *J. Mol. Biol.* (2009), doi:10.1016/j.jmb.2009.02.056

200, GE Healthcare) using 10 mM Tris–HCl, 50 mM KCl, and 1 mM DTT (pH 7.4) as elution buffer. hNS eluted as a single peak with an apparent molecular mass of 45 kDa.

hNS crystallization

Crystallization trials were performed by sitting-drop vapour-diffusion technique using an Oryx 8 crystallization robot (Douglas Instruments, East Garston, UK) at 293 °K. hNS yielded crystal hits under 23 different conditions. Optimization of crystal growth conditions were carried out by manual sitting-drop experiments. Crystals were grown by mixing equal volumes (1–2 μl) of hNS (13 mg/ml) and precipitant solution. The best-diffracting crystals appeared within 2 weeks in 1.4 M ammonium sulfate and 0.1 M sodium cacodylate, pH 6.3 (293 °K). Before data collection, the crystals were flash-frozen in liquid nitrogen with the use of a cryoprotectant solution containing 25% glycerol in the crystallization buffer. Data collection was performed at 110 K on beam line ID14-2 at the European Synchrotron Radiation Facility (ESRF) (Grenoble, France).

Native neuroserpin: structure determination and refinement

X-ray diffraction data were processed with MOSFLM and SCALA.[37,38] A partial molecular replacement solution was obtained with BALBES,[39] which could locate four hNS molecules, using human alpha1 antitrypsin as search model. Notably, when the hNS sequence was used as input to BALBES, the program failed to find a solution, while forcing the use of alpha1 antitrypsin sequence prevented BALBES to base the search model ensemble on the murine-cleaved neuroserpin structure. Only after thorough manual model building with COOT[40] and structure refinement with REFMAC5[41] did the electron density for the fifth hNS molecule become apparent, and the molecule was properly located by MOLREP.[42] Restrained and 'tls' refinement procedures were applied. Non-crystallographic symmetry restrains were applied to all the five molecules, with the exception of the RCLs and the 258–283 region of molecule C. Protein–protein interaction analysis was carried out through the PROTORP server.[43]

Limited proteolysis and crystallization of cleaved hNS

Human neuroserpin at the concentration of 9 mg/ml was incubated for 1 h at 37 °C with trypsin (Sigma), applying a 1:10 protease–hNS concentration ratio. The proteolytic reaction was blocked by prompt addition of soybean trypsin inhibitor (Sigma) at the final concentration of 3.3 mg/ml. Cleaved hNS was washed by size-exclusion chromatography using a Sephadex 200 10/300 GL column (GE Healthcare) and by elution with 10 mM Tris–HCl, 50 mM KCl, and 1 mM DTT (pH 7.4). Cleaved hNS was concentrated to a final concentration of 13.8 mg/ml before crystallization. Crystallization trials were performed using an Oryx 8 crystallization robot (Douglas Instruments) at 293 K. Crystals of diffraction quality were found in the F1 condition of Hampton Research crystal screen [0.2 M ammonium sulfate, 0.1 M sodium acetate (pH 4.6), 30% PEG (polyethylene glycol) MME 2000] after 4 weeks. Crystals were flash-frozen using their unmodified mother liquor as cryoprotectant.

Cleaved hNS: structure determination and refinement

X-ray diffraction data were collected at the beam line ID14-1 (ESRF Grenoble). Data were then processed using MOSFLM and SCALA.[37,38] One molecule of cleaved mouse neuroserpin (PDB code 1JJO)[23] was adopted as search model for molecular replacement using PHASER and MOLREP.[42,44] Despite several trials, both programs were able to locate only one of the two expected asymmetric unit molecules. After refinement of this partial solution (at 1.85 Å resolution), ARP-WARP[45] was used to automatically build a 90% complete model of the second chain; further manual model building was then carried out using COOT.[40] The cleaved hNS structure was refined using REFMAC5, applying maximum likelihood residual, anisotropic scaling, bulk-solvent correction, and atomic displacement parameter refinement using the 'tls' method.[41] Figures were produced using PyMOL§ and CCP4mg.[46] The electrostatic potential was calculated with PyMOL and APBS,[47] where solvent dielectric contribution (the dielectric constants applied were 80 for the solvent and 8 and 4 for the protein) was taken into account. The ionic concentration was set to 0.15 M.

Determination of inhibition rate constants

The rate constants for the inhibitory reaction between hNS and two-chain tPA (American Diagnostica) were determined in the presence of the chromogenic substrate IPR-pNA (Chromogenix) by analyzing the progress curves for the formation of pNA upon cleavage of the substrate. Experiments were performed at 298 K in 50 mM Tris, 10 mM Na_2HPO_4, 150 mM NaCl, and 0.1% Tween (pH 7.4). Buffer, inhibitor (15, 30, 60, 120, and 240 nM), and substrate (170 μM) were mixed in a 2-ml cuvette and reactions were initiated by addition of a fixed amount of tPA (1 nM). Product accumulation was continuously recorded by a Cary 4E spectrophotometer (Varian, Inc.) at 405 nm. A typical experiment consisted of six assays (one zero and five non-zero hNS concentrations). The progress curve data were simultaneously fitted according to the minimal kinetic scheme [Eq. (1)]:

$$\begin{aligned} &\mathrm{tPA} + \mathrm{hNS} \underset{k_{-1}}{\overset{k_1}{\longleftrightarrow}} \mathrm{hNS-tPA} \xrightarrow{k_2} \mathrm{hNS4/tPA} \xrightarrow{k_{bk}} \mathrm{tPA} + \mathrm{hNS}^* \quad \text{reaction 1} \\ &\mathrm{tPA} + \mathrm{S} \overset{TS\,K_m}{\longleftrightarrow} \mathrm{tPA-S} \overset{TS\,K_{cat}}{\longrightarrow} \mathrm{tPA} + \mathrm{P} \quad \text{reaction 2} \end{aligned} \tag{1}$$

where hNS stands for human neuroserpin, hNS-tPA is the Michaelis intermediate of the enzyme inhibitor interaction, hNS∗/tPA is the acyl–enzyme intermediate, and hNS∗ is the cleaved hNS.

The resulting system of rate equations was solved through numerical integration by the software package COPASI 4.4.27 without any need for approximations.[48] A parameter search was run to decouple the values of the rates governing the hNS inhibitory reaction. The values of the apparent second-order inhibition constant (k_{inh}) and the rate constant for acyl–enzyme complex breakdown (k_{bk}) were calculated. Values for the rates of IPR-pNA hydrolysis were determined independently from the experiments in the absence of hNS.

§ http://pymol.sourceforge.net

Please cite this article as: Ricagno, S. *et al.*, Human Neuroserpin: Structure and Time-Dependent Inhibition, *J. Mol. Biol.* (2009), doi:10.1016/j.jmb.2009.02.056

Plasminogen activation in the presence of recombinant hNS

The rate of Lys-plasminogen (American Diagnostica) activation by tPA in the presence of recombinant hNS was measured by an indirect assay using a chromogenic substrate specific for plasmin (Pyro-Glu-Phe-Lys-*p*-nitroanilide, EFK-pNA). Buffer, hNS (200, 400, and 800 nM), plasminogen (5 nM), and substrate (15 μM) were mixed in a 2-ml cuvette and reactions were initiated by addition of a fixed amount of tPA (20 nM). In this assay, the release of pNA depends on four reactions: (1) the inhibition of tPA by hNS (reaction 1), (2) the activation of plasminogen to plasmin by tPA (reaction 3), (3) the cleavage of hNS by plasmin (reaction 4), and (4) the cleavage of EFK-pNA by plasmin (reaction 5):

$$\mathrm{tPA} + \mathrm{hNS} \underset{k_{-1}}{\overset{k_1}{\longleftrightarrow}} \mathrm{hNS{-}tPA} \xrightarrow{k_2} \mathrm{hNS4/tPA} \xrightarrow{k_{bk}} \mathrm{tPA} + \mathrm{hNS^*} \quad \text{reaction 2}$$

$$\mathrm{tPA} + \mathrm{Plg} \overset{^{T}K_m}{\longleftrightarrow} \mathrm{tPA{-}Plg} \overset{^{T}K_{cat}}{\longrightarrow} \mathrm{tPA} + \mathrm{PI} \quad \text{reaction 3}$$

$$\mathrm{PI} + \mathrm{NS} \overset{^{P}K_m}{\longleftrightarrow} \mathrm{PI{-}NS} \overset{^{P}K_{cat}}{\longrightarrow} \mathrm{PI} + \mathrm{NS^*} \quad \text{reaction 4}$$

$$\mathrm{PI} + \mathrm{EFK{-}pNA} \overset{^{PS}K_m}{\longleftrightarrow} \mathrm{PI{-}EFK{-}pNA} \overset{^{PS}K_{cat}}{\longrightarrow} \mathrm{PI} + \mathrm{pNA} \quad \text{reaction 5}$$

Under the chosen conditions, the progress curves of EFK-pNA hydrolysis were very sensitive to the specificity constant (k_{cat}/K_m) for plasminogen activation by tPA. The reactions 1, 3, and 5 were studied directly in separate experiments, and the rate constants obtained were constrained in the global fitting. Analogously, no direct hydrolysis of EFK-pNA by tPA was measured. The kinetics of plasmin generation was then calculated.

Formation and deacylation of hNS*/tPA acyl–enzyme complex

Samples at varying hNS *versus* tPA concentrations (6:1, 4:1, and 2:1 ratios) were incubated in the same buffer used for the chromogenic assays. The reactions were stopped at time intervals by addition of SDS sample buffer containing β-mercaptoethanol followed by 10 min boiling. Products and reagents were separated by SDS-PAGE analysis in 10% separating polyacrylamide gels. After electrophoresis, proteins were stained with SYPRO Ruby (Molecular Probes), visualized by means of a Typhoon 9200 laser scanner, and quantified with the ImageQUANT software (GE Healthcare Life Science). SYPRO Ruby is an ultrasensitive fluorescent stain with a wide linear range for protein quantization, which allowed an accurate quantification of the protein content of each band. The data arising from the kinetics of intact, complexed, and cleaved inhibitor were fitted according to reaction 1.

Protein Data Bank accession numbers

Atomic coordinates and structure factors for native and cleaved hNS (PDB codes 3F5N and 3F02, respectively) have been deposited with the PDB.‖

‖ http://www.rcsb.org

Acknowledgements

We are grateful to Prof. David Lomas and Dr. Didier Belorgey (University of Cambridge, UK) for providing the hNS plasmid, Prof. Paolo Ascenzi (University of Roma Tre, Italy) for helpful discussion, and Raffaele Cerutti for technical help. This work was supported by grants from the Cariplo Foundation (GUARD Project, 2006–2009) and the Italian Ministry of University and Research (Italy; FIRB Project "Biologia Strutturale"). We further thank Drs. Gerard Bricogne and Thomas Womack (Global Phasing, Cambridge, UK) for helpful advice during the early stages of this work.

Supplementary Data

Supplementary data associated with this article can be found, in the online version, at doi:10.1016/j.jmb.2009.02.056

References

1. Miranda, E. & Lomas, D. A. (2006). Neuroserpin: a serpin to think about. *Cell. Mol. Life Sci.* **63**, 709–722.
2. Hastings, G. A., Coleman, T. A., Haudenschild, C. C., Stefansson, S., Smith, E. P., Barthlow, R. *et al.* (1997). Neuroserpin, a brain-associated inhibitor of tissue plasminogen activator is localized primarily in neurons. Implications for the regulation of motor learning and neuronal survival. *J. Biol. Chem.* **272**, 33062–33067.
3. Silverman, G. A., Bird, P. I., Carrell, R. W., Church, F. C., Coughlin, P. B., Gettins, P. G. *et al.* (2001). The serpins are an expanding superfamily of structurally similar but functionally diverse proteins. Evolution, mechanism of inhibition, novel functions, and a revised nomenclature. *J. Biol. Chem.* **276**, 33293–33296.
4. Lee, T. W., Coates, L. C. & Birch, N. P. (2008). Neuroserpin regulates *N*-cadherin-mediated cell adhesion independently of its activity as an inhibitor of tissue plasminogen activator. *J. Neurosci. Res.* **86**, 1243–1253.
5. Osterwalder, T., Cinelli, P., Baici, A., Pennella, A., Krueger, S. R., Schrimpf, S. P. *et al.* (1998). The axonally secreted serine proteinase inhibitor, neuroserpin, inhibits plasminogen activators and plasmin but not thrombin. *J. Biol. Chem.* **273**, 2312–2321.
6. Kinghorn, K. J., Crowther, D. C., Sharp, L. K., Nerelius, C., Davis, R. L., Chang, H. T. *et al.* (2006). Neuroserpin binds Abeta and is a neuroprotective component of amyloid plaques in Alzheimer disease. *J. Biol. Chem.* **281**, 29268–29277.
7. Loebermann, H., Tokuoka, R., Deisenhofer, J. & Huber, R. (1984). Human alpha 1-proteinase inhibitor. Crystal structure analysis of two crystal modifications, molecular model and preliminary analysis of the implications for function. *J. Mol. Biol.* **177**, 531–557.
8. Wilczynska, M., Fa, M., Ohlsson, P. I. & Ny, T. (1995). The inhibition mechanism of serpins. Evidence that the mobile reactive center loop is cleaved in the native protease–inhibitor complex. *J. Biol. Chem.* **270**, 29652–29655.
9. Huntington, J. A., Read, R. J. & Carrell, R. W. (2000). Structure of a serpin–protease complex shows inhibition by deformation. *Nature*, **407**, 923–926.

Please cite this article as: Ricagno, S. *et al.*, Human Neuroserpin: Structure and Time-Dependent Inhibition, *J. Mol. Biol.* (2009), doi:10.1016/j.jmb.2009.02.056

10. Barker-Carlson, K., Lawrence, D. A. & Schwartz, B. S. (2002). Acyl–enzyme complexes between tissue-type plasminogen activator and neuroserpin are short-lived in vitro. *J. Biol. Chem.* **277**, 46852–46857.
11. Whisstock, J. C. & Bottomley, S. P. (2006). Molecular gymnastics: serpin structure, folding and misfolding. *Curr. Opin. Struct. Biol.* **16**, 761–768.
12. Zhou, A., Huntington, J. A., Pannu, N. S., Carrell, R. W. & Read, R. J. (2003). How vitronectin binds PAI-1 to modulate fibrinolysis and cell migration. *Nat. Struct. Biol.* **10**, 541–544.
13. Zhang, Q., Buckle, A. M., Law, R. H., Pearce, M. C., Cabrita, L. D., Lloyd, G. J. *et al.* (2007). The N terminus of the serpin, tengpin, functions to trap the metastable native state. *EMBO Rep.* **8**, 658–663.
14. Lomas, D. A., Evans, D. L., Finch, J. T. & Carrell, R. W. (1992). The mechanism of Z alpha 1-antitrypsin accumulation in the liver. *Nature*, **357**, 605–607.
15. Lomas, D. A., Belorgey, D., Mallya, M., Miranda, E., Kinghorn, K. J., Sharp, L. K. *et al.* (2005). Molecular mousetraps and the serpinopathies. *Biochem. Soc. Trans.* **33**, 321–330.
16. Whisstock, J. C. & Bottomley, S. P. (2008). Structural biology: serpins' mystery solved. *Nature*, **455**, 1189–1190.
17. Yamasaki, M., Li, W., Johnson, D. J. & Huntington, J. A. (2008). Crystal structure of a stable dimer reveals the molecular basis of serpin polymerization. *Nature*, **455**, 1255–1258.
18. Davis, R. L., Shrimpton, A. E., Carrell, R. W., Lomas, D. A., Gerhard, L., Baumann, B. *et al.* (2002). Association between conformational mutations in neuroserpin and onset and severity of dementia. *Lancet*, **359**, 2242–2247.
19. Miranda, E., MacLeod, I., Davies, M. J., Perez, J., Romisch, K., Crowther, D. C. & Lomas, D. A. (2008). The intracellular accumulation of polymeric neuroserpin explains the severity of the dementia FENIB. *Hum. Mol. Genet.* **17**, 1527–1539.
20. Miranda, E., Romisch, K. & Lomas, D. A. (2004). Mutants of neuroserpin that cause dementia accumulate as polymers within the endoplasmic reticulum. *J. Biol. Chem.* **279**, 28283–28291.
21. Takasawa, A., Kato, I., Takasawa, K., Ishii, Y., Yoshida, T., Shehata, M. H. *et al.* (2008). Mutation-, aging-, and gene dosage-dependent accumulation of neuroserpin (G392E) in endoplasmic reticula and lysosomes of neurons in transgenic mice. *J. Biol. Chem.* **283**, 35606–35613.
22. Coutelier, M., Andries, S., Ghariani, S., Dan, B., Duyckaerts, C., van Rijckevorsel, K. *et al.* (2008). Neuroserpin mutation causes electrical status epilepticus of slow-wave sleep. *Neurology*, **71**, 64–66.
23. Briand, C., Kozlov, S. V., Sonderegger, P. & Grutter, M. G. (2001). Crystal structure of neuroserpin: a neuronal serpin involved in a conformational disease. *FEBS Lett.* **505**, 18–22.
24. Gettins, P. G. (2002). Serpin structure, mechanism, and function. *Chem. Rev.* **102**, 4751–4804.
25. Morrison, J. F. & Walsh, C. T. (1988). The behavior and significance of slow-binding enzyme inhibitors. *Adv. Enzymol. Relat. Areas Mol. Biol.* **61**, 201–301.
26. Belorgey, D., Crowther, D. C., Mahadeva, R. & Lomas, D. A. (2002). Mutant neuroserpin (S49P) that causes familial encephalopathy with neuroserpin inclusion bodies is a poor proteinase inhibitor and readily forms polymers in vitro. *J. Biol. Chem.* **277**, 17367–17373.
27. Hill, R. M., Parmar, P. K., Coates, L. C., Mezey, E., Pearson, J. F. & Birch, N. P. (2000). Neuroserpin is expressed in the pituitary and adrenal glands and induces the extension of neurite-like processes in AtT-20 cells. *Biochem. J.* **345**, 595–601.
28. Johnson, D. J., Li, W., Adams, T. E. & Huntington, J. A. (2006). Antithrombin-S195A factor Xa-heparin structure reveals the allosteric mechanism of antithrombin activation. *EMBO J.* **25**, 2029–2037.
29. Makarova, A., Mikhailenko, I., Bugge, T. H., List, K., Lawrence, D. A. & Strickland, D. K. (2003). The low density lipoprotein receptor-related protein modulates protease activity in the brain by mediating the cellular internalization of both neuroserpin and neuroserpin-tissue-type plasminogen activator complexes. *J. Biol. Chem.* **278**, 50250–50258.
30. Gettins, P. G. (2002). The F-helix of serpins plays an essential, active role in the proteinase inhibition mechanism. *FEBS Lett.* **523**, 2–6.
31. Shin, J. S. & Yu, M. H. (2006). Viscous drag as the source of active site perturbation during protease translocation: insights into how inhibitory processes are controlled by serpin metastability. *J. Mol. Biol.* **359**, 378–389.
32. Zhou, A., Carrell, R. W. & Huntington, J. A. (2001). The serpin inhibitory mechanism is critically dependent on the length of the reactive center loop. *J. Biol. Chem.* **276**, 27541–27547.
33. Liu, L., Mushero, N., Hedstrom, L. & Gershenson, A. (2007). Short-lived protease serpin complexes: partial disruption of the rat trypsin active site. *Protein Sci.* **16**, 2403–2411.
34. Huber, R. & Carrell, R. W. (1989). Implications of the three-dimensional structure of alpha 1-antitrypsin for structure and function of serpins. *Biochemistry*, **28**, 8951–8966.
35. Ibarra, C. A., Blouse, G. E., Christian, T. D. & Shore, J. D. (2004). The contribution of the exosite residues of plasminogen activator inhibitor-1 to proteinase inhibition. *J. Biol. Chem.* **279**, 3643–3650.
36. Madison, E. L., Goldsmith, E. J., Gerard, R. D., Gething, M. J. & Sambrook, J. F. (1989). Serpin-resistant mutants of human tissue-type plasminogen activator. *Nature*, **339**, 721–724.
37. CCP4 (1994). The CCP4 suite: programs for protein crystallography. *Acta Crystallogr., Sect. D: Biol. Crystallogr.* **50**, 760–763.
38. Leslie, A. G. W. (1992). Recent changes to the MOSFLM package for processing film and image plate data. *Joint CCP4 + ESF-EACMB Newslett. Protein Crystallogr.* Q2
39. Long, F., Vagin, A. A., Young, P. & Murshudov, G. N. (2008). BALBES: a molecular replacement pipeline. *Acta Crystallogr., Sect. D: Biol. Crystallogr.* **64**, 125–132.
40. Emsley, P. & Cowtan, K. (2004). Coot: model-building tools for molecular graphics. *Acta Crystallogr., Sect. D: Biol. Crystallogr.* **60**, 2126–2132.
41. Murshudov, G. N., Vagin, A. A. & Dodson, E. J. (1997). Refinement of macromolecular structures by the maximum-likelihood method. *Acta Crystallogr., Sect. D: Biol. Crystallogr.* **53**, 240–255.
42. Vagin, A. A. & Teplyakov, A. (1997). MOLREP: an automated program for molecular replacement. *J. Appl. Crystallogr.*, 1022–1025. Q3
43. Reynolds, Damerell & Jones. Protorp: a protein–protein interaction analysis tool. Submitted. Q4
44. McCoy, A. J., Grosse-Kunstleve, R. W., Adams, P. D., Winn, M. D., Storoni, L. C. & Read, R. J. (2007). Phaser crystallographic software. *J. Appl. Crystallogr.* **40**, 658–674.

Please cite this article as: Ricagno, S. *et al.*, Human Neuroserpin: Structure and Time-Dependent Inhibition, *J. Mol. Biol.* (2009), doi:10.1016/j.jmb.2009.02.056

45. Morris, R. J., Perrakis, A. & Lamzin, V. S. (2003). ARP/wARP and automatic interpretation of protein electron density maps. *Methods Enzymol.* **374**, 229–244.
46. Potterton, L., McNicholas, S., Krissinel, E., Gruber, J., Cowtan, K., Emsley, P. *et al.* (2004). Developments in the CCP4 molecular-graphics project. *Acta Crystallogr., Sect. D: Biol. Crystallogr.* **60**, 2288–2294.
47. Baker, N. A., Sept, D., Joseph, S., Holst, M. J. & McCammon, J. A. (2001). Electrostatics of nanosystems: application to microtubules and the ribosome. *Proc. Natl Acad. Sci. USA*, **98**, 10037–10041.
48. Hoops, S., Sahle, S., Gauges, R., Lee, C., Pahle, J., Simus, N. *et al.* (2006). COPASI—a COmplex PAthway SImulator. *Bioinformatics*, **22**, 3067–3074.

Please cite this article as: Ricagno, S. *et al.*, Human Neuroserpin: Structure and Time-Dependent Inhibition, *J. Mol. Biol.* (2009), doi:10.1016/j.jmb.2009.02.056